**Supplementary material**

# Histone lactylation-boosted ALKBH3 potentiates tumor progression and diminished promyelocytic leukemia protein nuclear condensates by m$^1$A demethylation of SP100

Xiang Gu[#], Ai Zhuang[#], Jie Yu[#], Ludi Yang[#], Shengfang Ge, Jing Ruan, Renbing Jia[*], Xianqun Fan[*], Peiwei Chai[*]

Department of Ophthalmology, Shanghai Key Laboratory of Orbital Diseases and Ocular Oncology, Shanghai Ninth People's Hospital, Shanghai Jiao Tong University School of Medicine, Shanghai, 20025, People's Republic of China.

[#]These authors contributed equally to this work.

[*]Corresponding author: renbingjia@sjtu.edu.cn (R.J.); fanxq@sjtu.edu.cn (X.F.); chaipeiwei123@sjtu.edu.cn (P.C.).

**Supplementary material files include 15 Figures and 7 Tables**

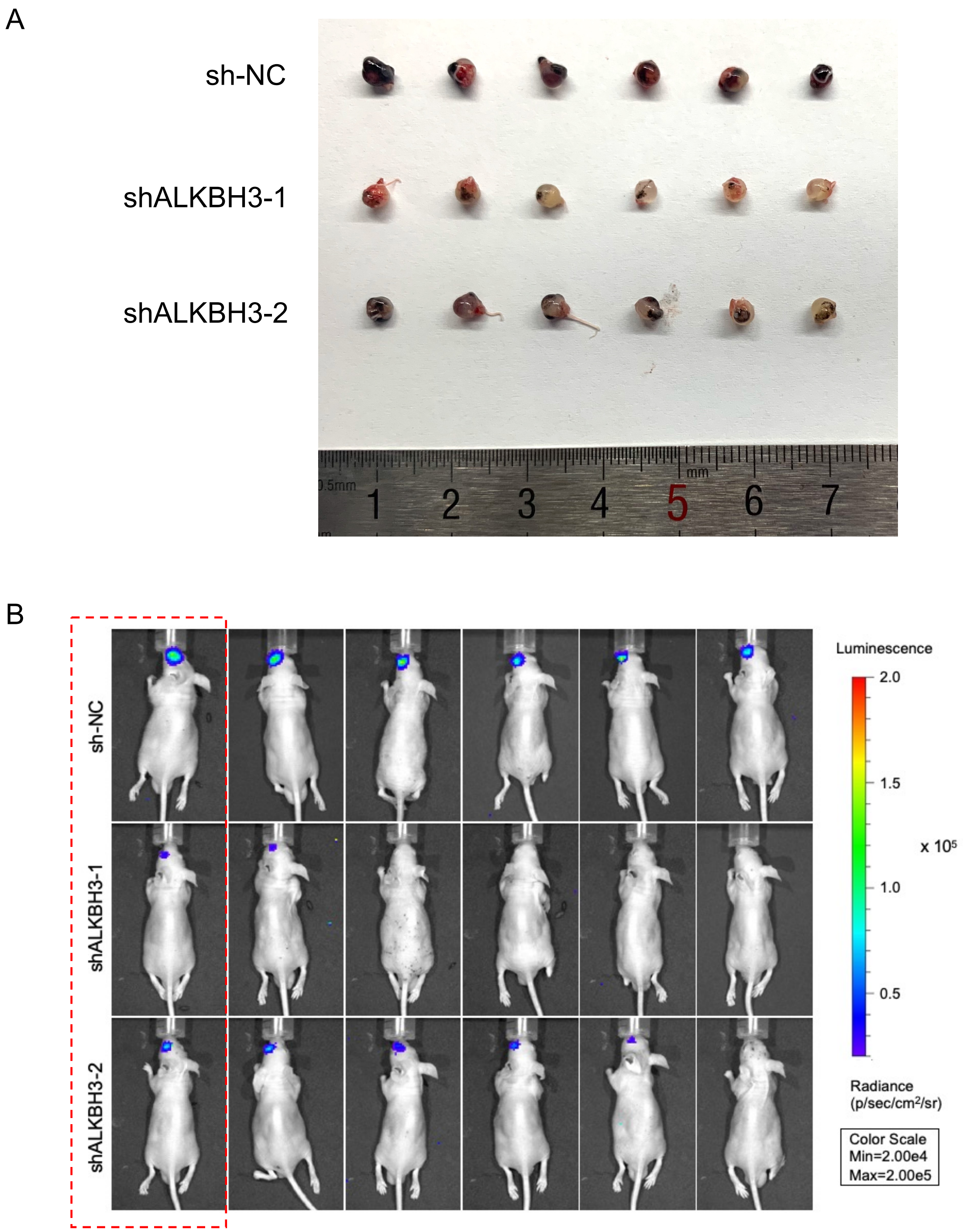

**Supplementary Figure S1.** ALKBH3 knockdown inhibited ocular melanoma tumorigenesis in vivo. (**A**) Images showing suppression of tumors in orthotopic xenografts derived from ALKBH3-deficient 92.1 cells. The data were obtained from six experimental replicates. (**B**) Images acquired with the small animal imaging system showing suppression of bioluminescent signals in orthotopic xenografts derived from ALKBH3-deficient 92.1 cells. The data were obtained from six experimental replicates.

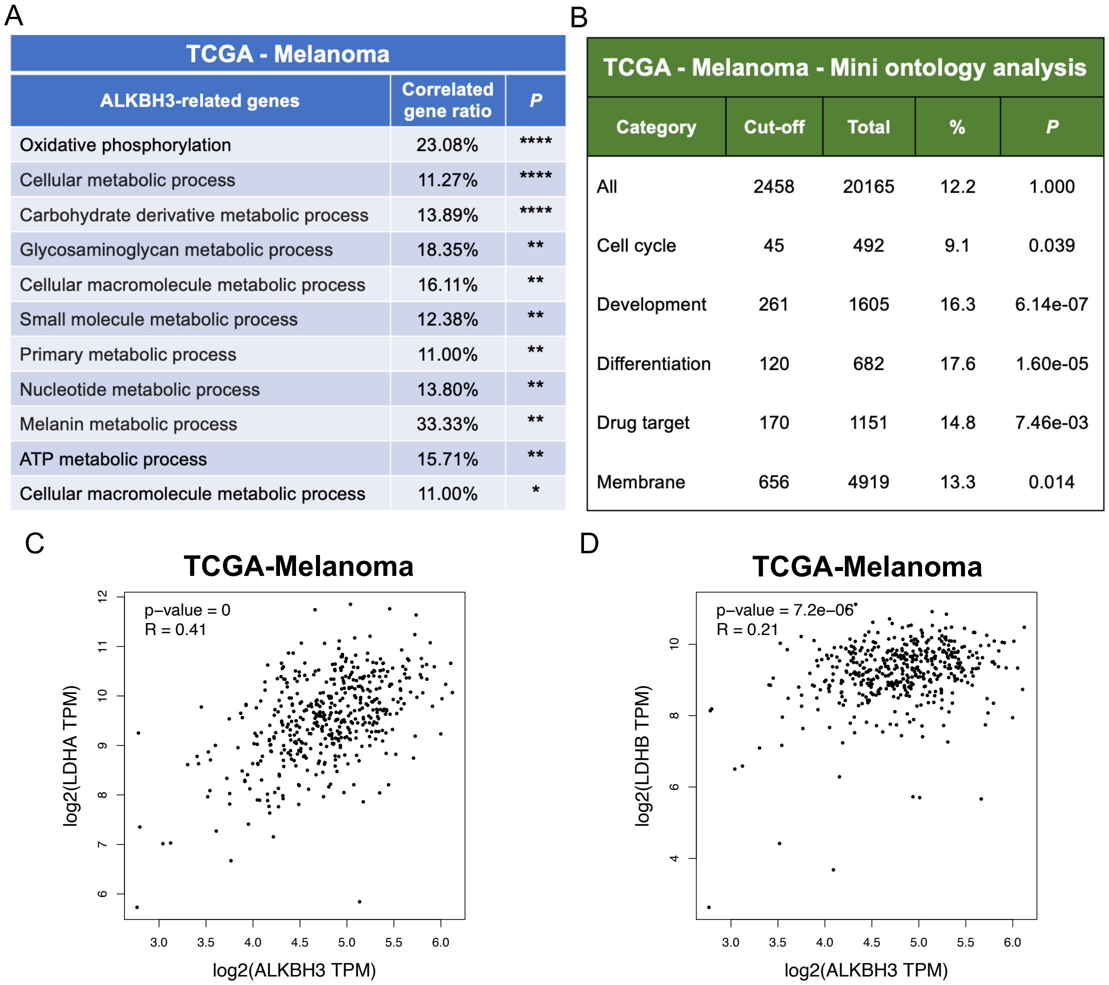

**TCGA - Melanoma**

| ALKBH3-related genes | Correlated gene ratio | *P* |
|---|---|---|
| Oxidative phosphorylation | 23.08% | **** |
| Cellular metabolic process | 11.27% | **** |
| Carbohydrate derivative metabolic process | 13.89% | **** |
| Glycosaminoglycan metabolic process | 18.35% | ** |
| Cellular macromolecule metabolic process | 16.11% | ** |
| Small molecule metabolic process | 12.38% | ** |
| Primary metabolic process | 11.00% | ** |
| Nucleotide metabolic process | 13.80% | ** |
| Melanin metabolic process | 33.33% | ** |
| ATP metabolic process | 15.71% | ** |
| Cellular macromolecule metabolic process | 11.00% | * |

**TCGA - Melanoma - Mini ontology analysis**

| Category | Cut-off | Total | % | *P* |
|---|---|---|---|---|
| All | 2458 | 20165 | 12.2 | 1.000 |
| Cell cycle | 45 | 492 | 9.1 | 0.039 |
| Development | 261 | 1605 | 16.3 | 6.14e-07 |
| Differentiation | 120 | 682 | 17.6 | 1.60e-05 |
| Drug target | 170 | 1151 | 14.8 | 7.46e-03 |
| Membrane | 656 | 4919 | 13.3 | 0.014 |

**Supplementary Figure S2.** ALKBH3-related genes are enriched in metabolic terms. (**A**) GO analysis of ALKBH3-related genes in the TCGA-Melanoma cohort (n=470). (**B**) Mini ontology analysis of ALKBH3-related genes in the TCGA-Melanoma cohort. (**C** and **D**) Correlation analysis of ALKBH3 expression and LDHA (**C**) or LDHB (**D**) expression in the TCGA-Melanoma cohort. Significance was determined by *Pearson* correlation analysis (LDHA: R = 0.41, LDHB: R = 0.21).

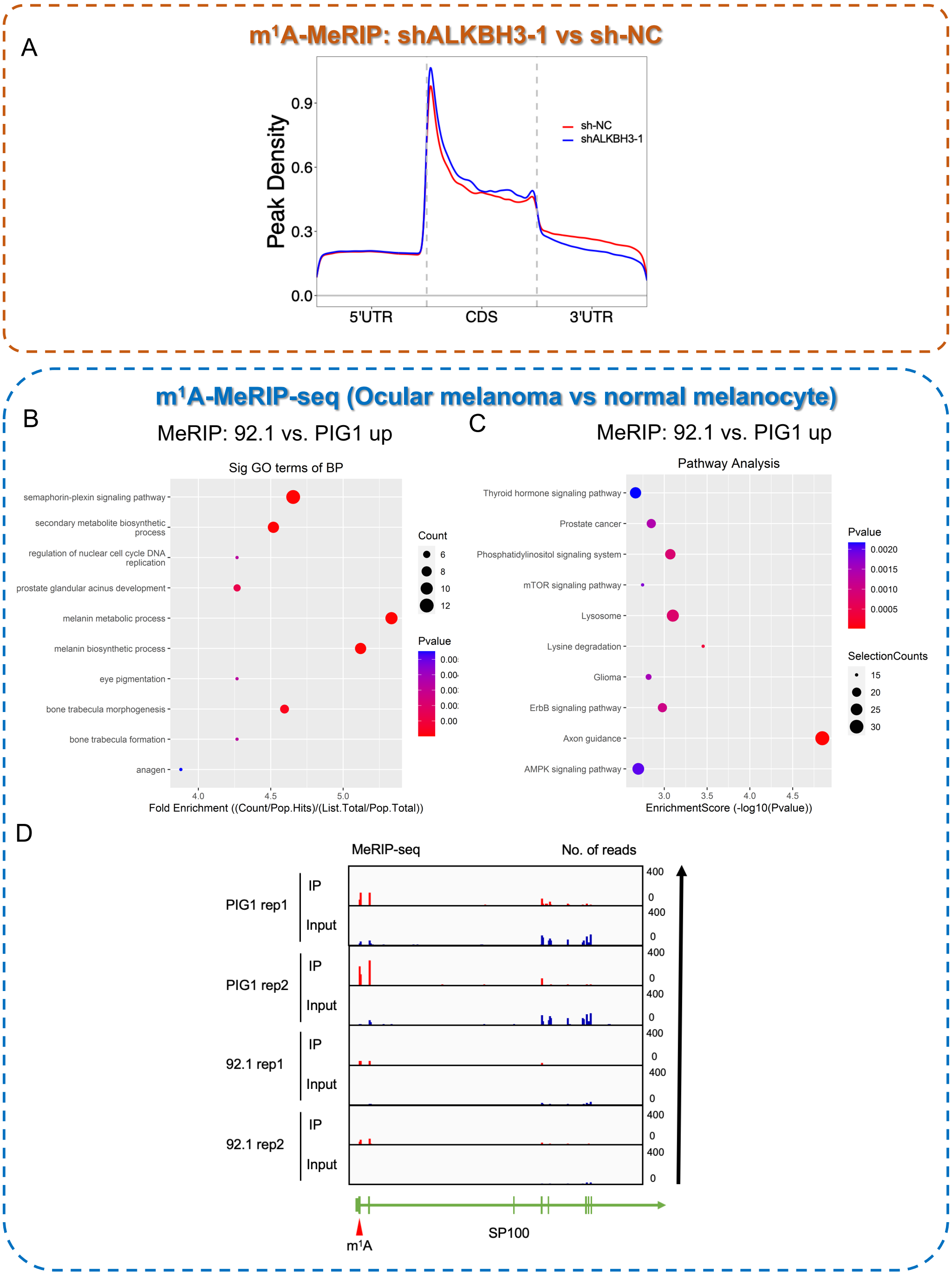

**Supplementary Figure S3.** m$^1$A-modified genes were associated with tumor-related pathways. (**A**) m$^1$A-meRIP-seq data showing the peak density of m$^1$A sites. Biological duplicates were analyzed. (**B**) GO analysis of m$^1$A-modified genes in ocular melanoma cells and normal melanocytes. (**C**) KEGG pathway analysis of m$^1$A-modified genes in ocular melanoma cells and normal melanocytes. (**D**) IGV tracks from m$^1$A-meRIP-seq analysis showing m$^1$A enrichment at the 5'UTR of SP100. Biological duplicates were analyzed.

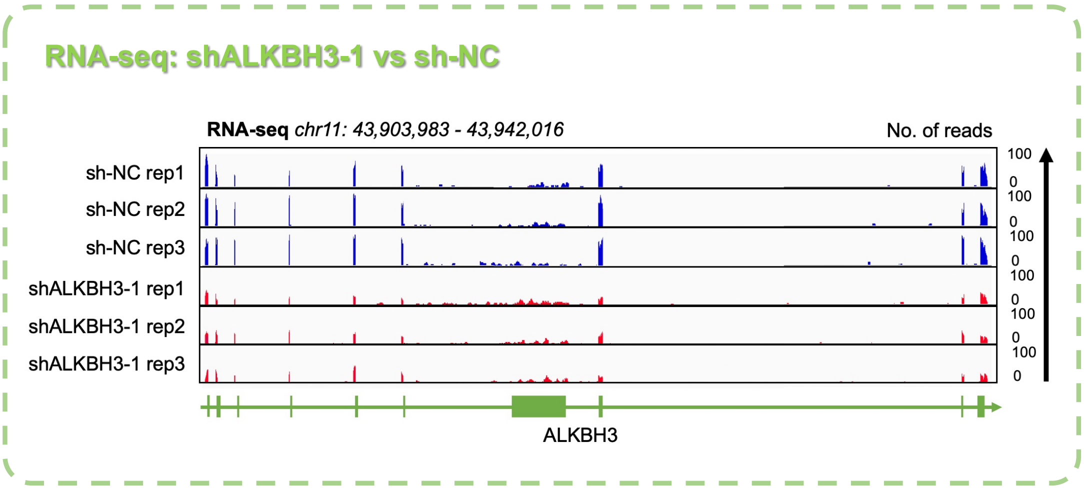

**Supplementary Figure S4.** The expression of ALKBH3 upon ALKBH3 knockdown. IGV tracks from RNA-seq analysis showing ALKBH3 expression in wild-type and ALKBH3-deficient ocular melanoma cells. Biological triplicates were analyzed.

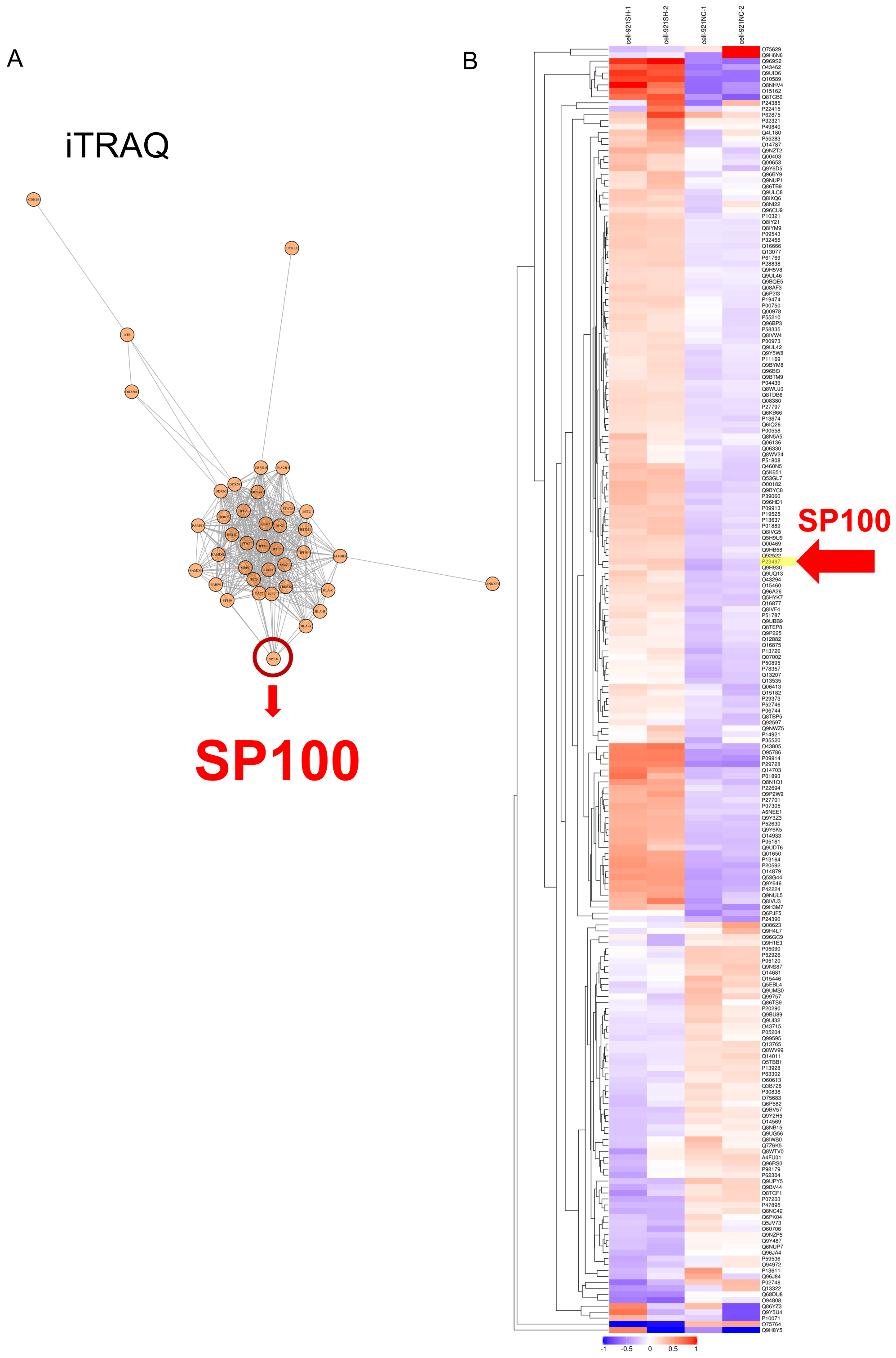

**Supplementary Figure S5.** SP100 presented with increased protein levels in ALKBH3-deficient cells. (**A**) Protein-protein interaction network analysis showing the protein expression of ALKBH3-regulated genes in wild-type and ALKBH3-deficient ocular melanoma cells. (**B**) Heatmap showing the differentially expressed proteins in wild-type and ALKBH3-deficient ocular melanoma cells.

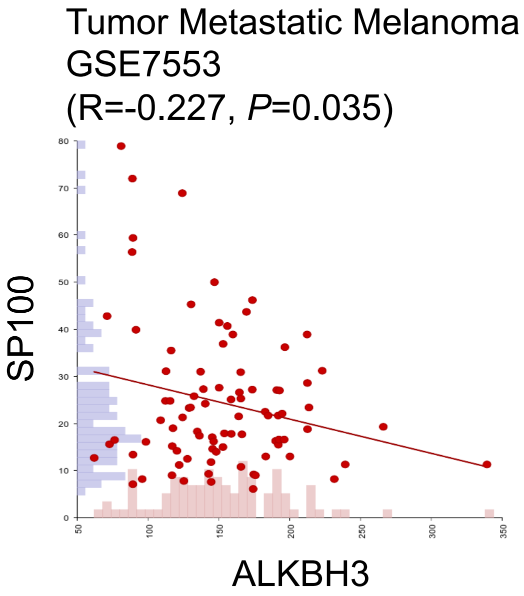

**Supplementary Figure S6.** The expression of SP100 was negatively associated with the expression of ALKBH3. Correlation analysis of ALKBH3 expression and SP100 expression in a cohort of metastatic melanoma samples (n=87). Significance was determined by *Pearson* correlation analysis (R = -0.227, *P* = 0.035).

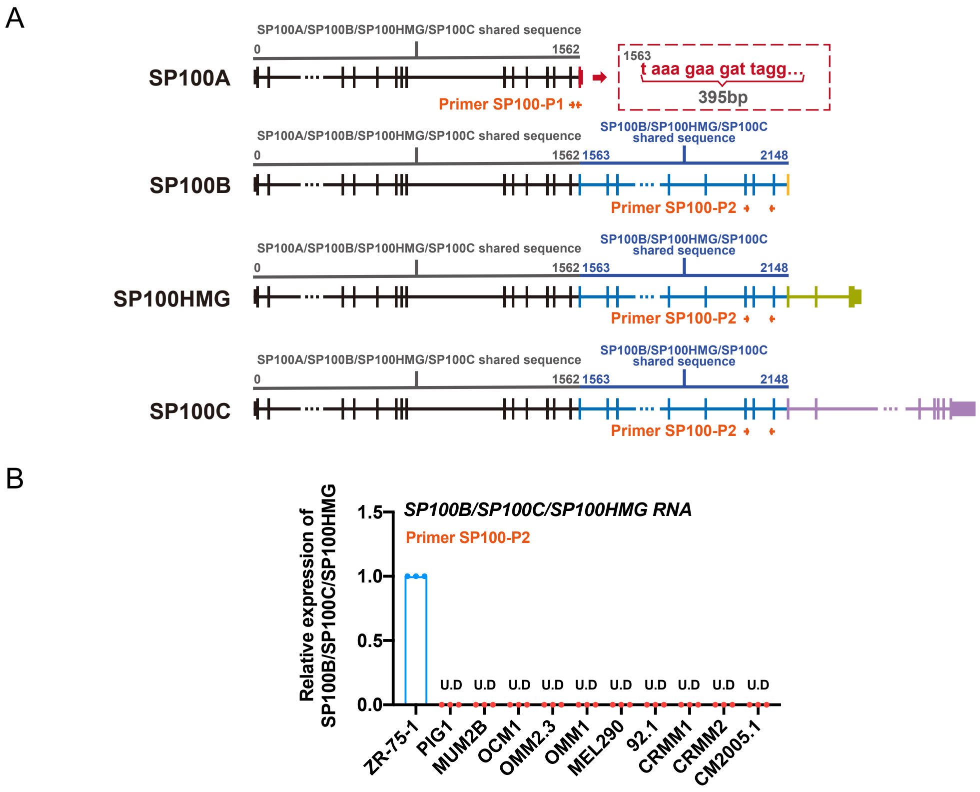

**Supplementary Figure S7.** The RNA expression of SP100B/SP100C/SP100HMG in ocular melanoma and normal melanocytes. (**A**) Sequence of SP100 isoforms. (**B**) qPCR data showing the SP100B/SP100C/SP100HMG expression in ocular melanoma cells, PIG1 cells relative to ZR-75–1 cell. The data are presented as the mean ± SD of experimental triplicates. U.D: undetected.

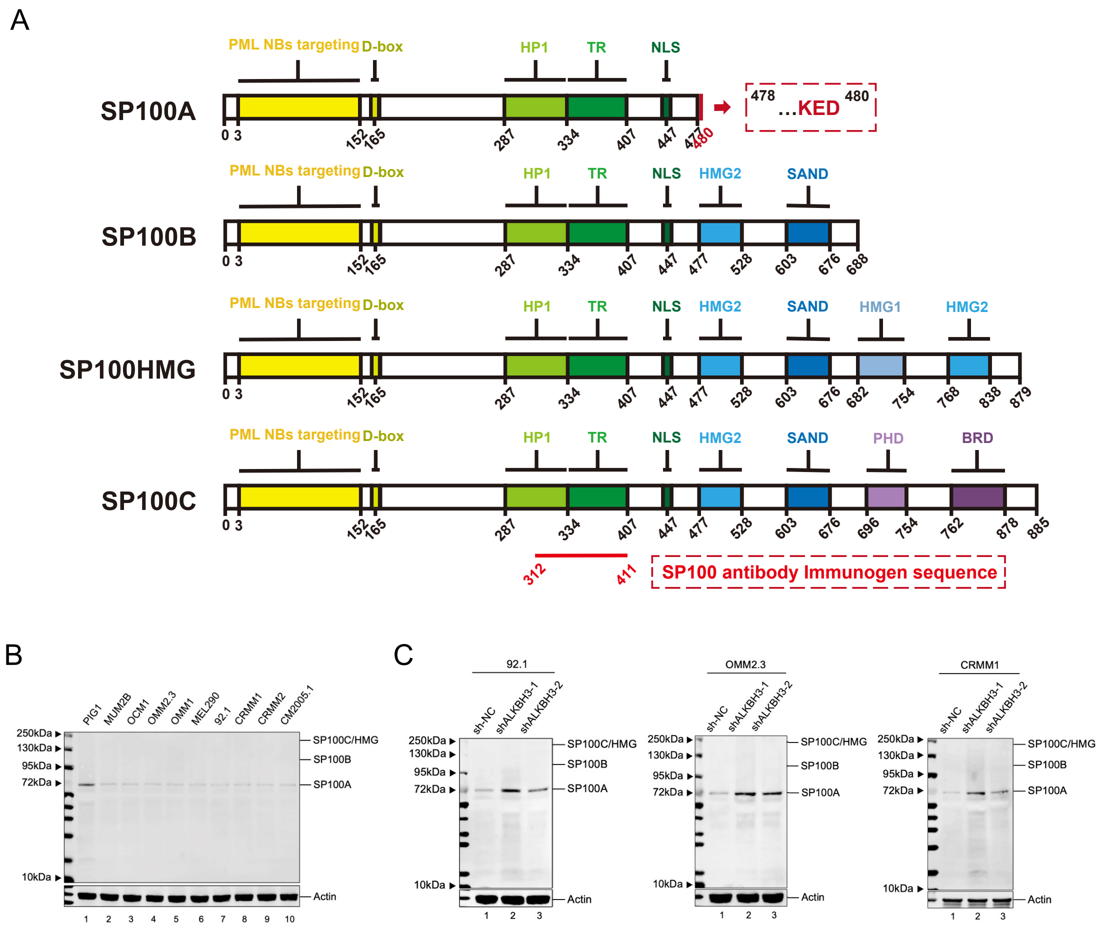

**Supplementary Figure S8.** The protein expression of SP100A, SP100B, SP100C and SP100HMG in ocular melanoma and normal melanocytes. (**A**) Protein domains of SP100 isoforms. D-box: Destruction-box (D-box); TR: trans-activating region; HMG: high mobility group; BRD: bromodomain; PHD: plant homeodomain. (**B**) Western blot showing SP100A, SP100B, SP100C and SP100HMG expression relative to ACTB expression in ocular melanoma cells (MUM2B, OCM1, OMM2.3, OMM1, MEL290, 92.1, CRMM1, CRMM2, CM2005.1) and normal pigmented cells (PIG1). The data are representative of experimental triplicates. (**C**) Western blot showing SP100A, SP100B, SP100C and SP100HMG expression relative to ACTB expression in wild-type and ALKBH3-deficient ocular melanoma cells (92.1, OMM2.3 and CRMM1).

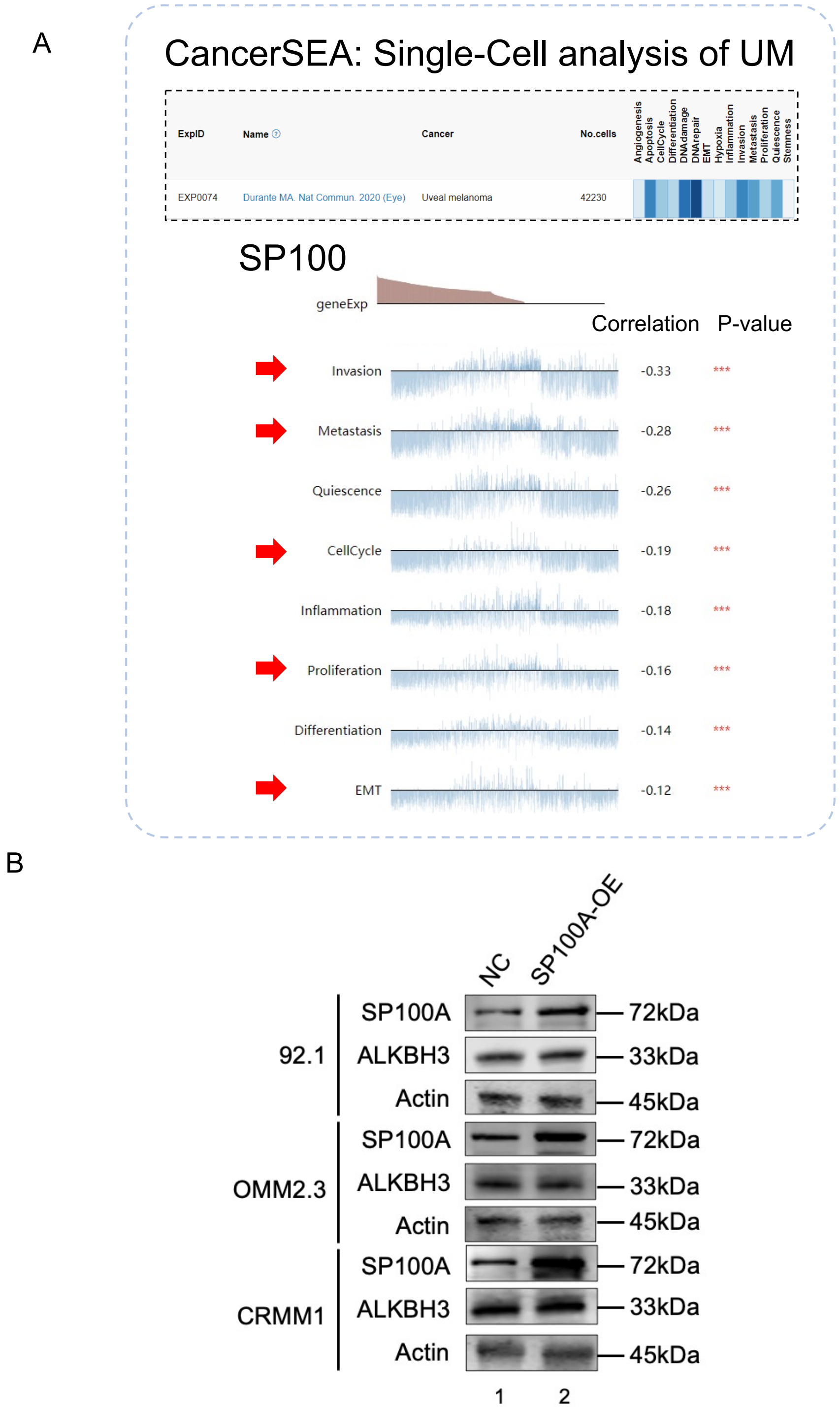

**Supplementary Figure S9.** SP100 prevents various oncogenic events in ocular melanoma. (**A**) Single-cell analysis data for ocular melanoma samples showing the correlation of SP100 expression and cancer-activation hallmarks using the CancerSEA platform. (**B**) Western blot showing SP100A and ALKBH3 expression relative to ACTB expression in ocular melanoma cells (92.1, OMM2.3 and CRMM1) upon SP100A overexpression. The data are representative of experimental triplicates.

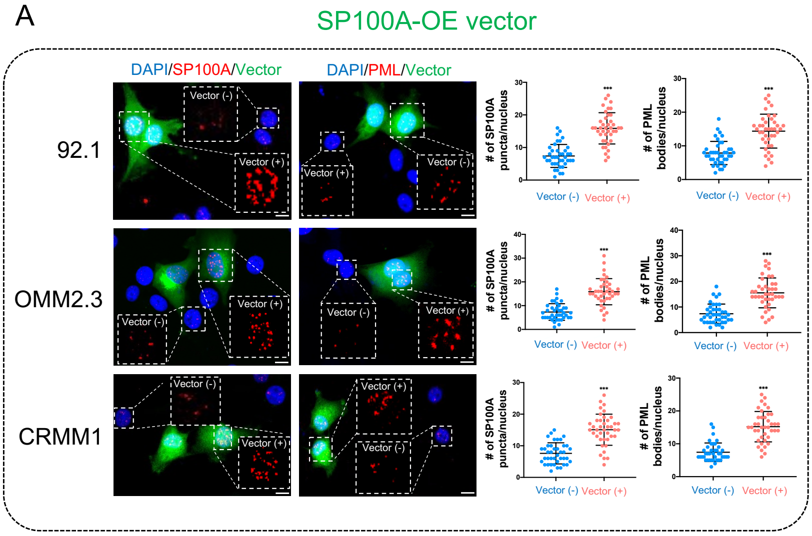

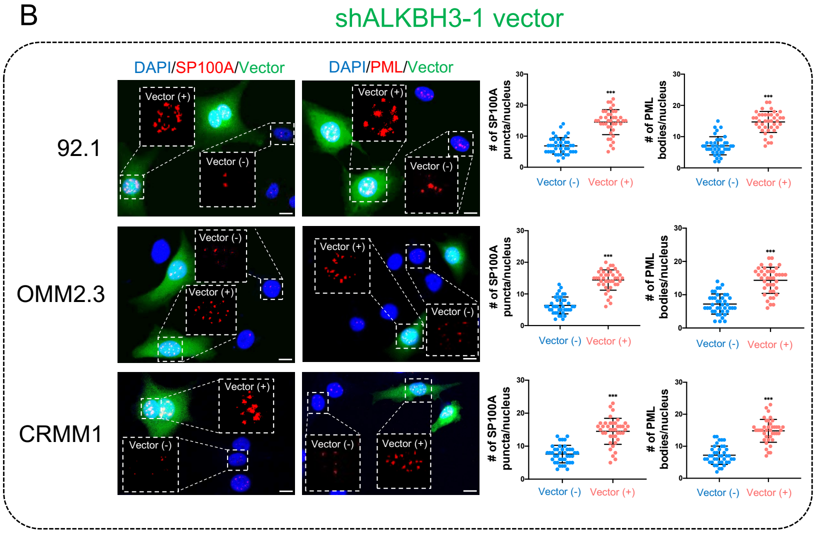

**Supplementary Figure S10.** Immunofluorescence analysis of the PML protein level through overexpressing SP100A and silencing of ALKBH3. (**A**) Immunofluorescence of Vector (green), SP100A (red), PML (red), and DAPI (blue) in ocular melanoma cells (92.1, OMM2.3 and CRMM1) upon SP100A overexpression. Scale bars: 10 μm. Number of SP100A puncta and PML bodies per nucleus (n = 40 cells) was quantified. Significance was determined by unpaired two-tailed Student's t test. *****P* < 0.0001. (**B**) Immunofluorescence of Vector (green), SP100A (red), PML (red), and DAPI (blue) in ocular melanoma cells (92.1, OMM2.3 and CRMM1) upon ALKBH3 knockdown. Scale bars: 10 μm. Number of SP100A puncta and PML bodies per nucleus (n = 40 cells) was quantified. Significance was determined by unpaired two-tailed Student's t test. *****P* < 0.0001.

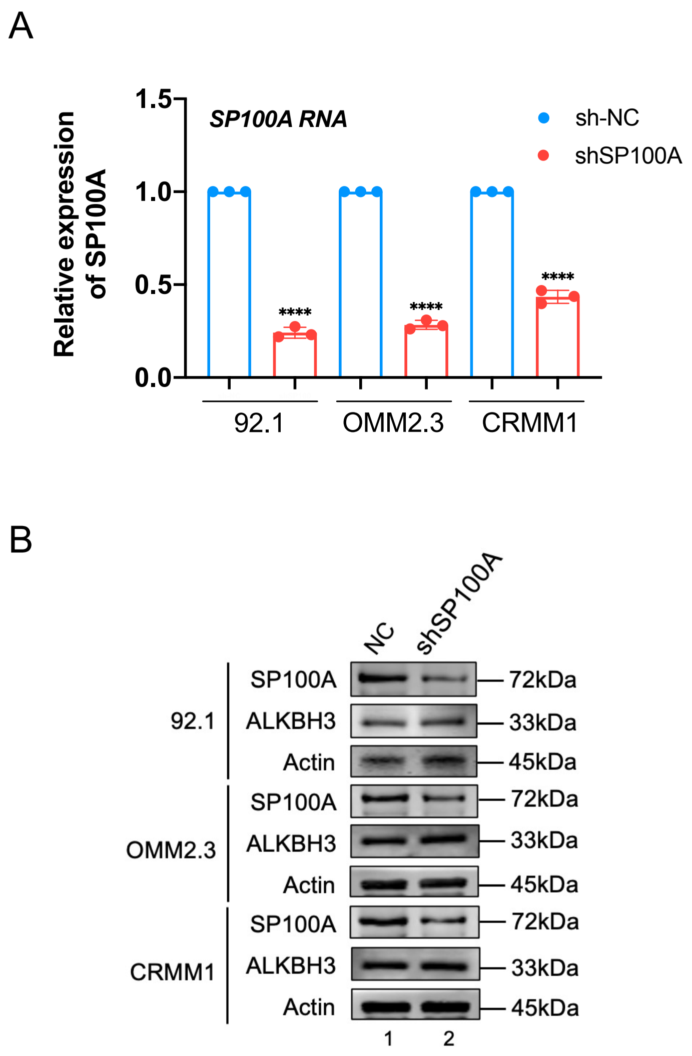

**Supplementary Figure S11.** SP100A presented with decreased expression in SP100A-deficient cells. (**A**) qPCR data showing the SP100A expression in ocular melanoma cells (92.1, OMM2.3 and CRMM1) upon SP100A knockdown. The data are presented as the mean ± SD of experimental triplicates. Significance was determined by unpaired two-tailed Student's t test. ****$P < 0.0001$. (**B**) Western blot of SP100A and ALKBH3 relative to ACTB in ocular melanoma cells (92.1, OMM2.3 and CRMM1) upon SP100A knockdown.

A

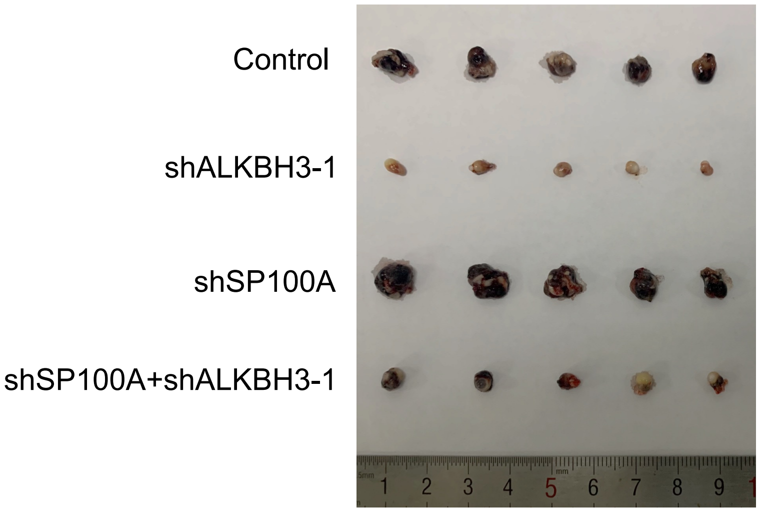

B

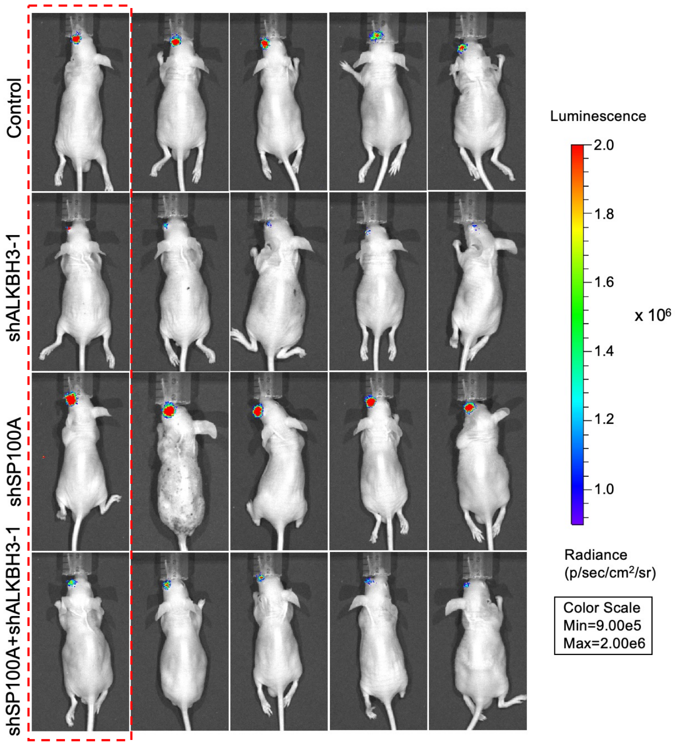

**Supplementary Figure S12.** The anticancer effects of ALKBH3 knockdown were partially blocked by SP100A silencing in vivo. (**A**) Images showing suppression of the growth of orthotopic xenografts tumors derived from ALKBH3-deficient 92.1 cells upon SP100 silencing. The data were obtained from five experimental replicates. (**B**) Images acquired with the small animal imaging system showing suppression of bioluminescent signals in orthotopic xenografts derived from ALKBH3-deficient 92.1 cells upon SP100A silencing. The data were obtained from five experimental replicates.

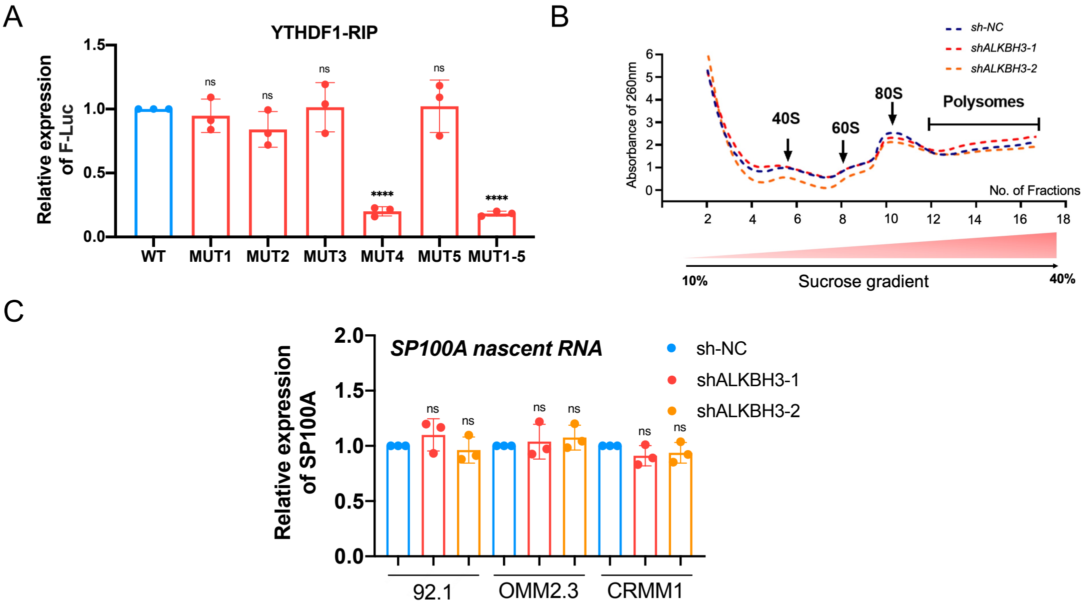

**Supplementary Figure S13.** Analysis of RNA fate of SP100A. (**A**) RIP-qPCR assay demonstrated the relative F-luc expression of the wild-type and six mutant SP100A 5’UTR reporter vectors by YTHDF1. The data are presented as the mean ± SD of experimental triplicates. Significance was determined by unpaired two-tailed Student’s *t* test. *****P* < 0.0001. (**B**) Polysome profiling assays upon ALKBH3 knockdown. Fractionation of lysates from 92.1 cells with or without ALKBH3 knockdown. Significance was determined by unpaired two-tailed Student’s *t* test. ****P* < 0.001, *****P* < 0.0001. (**C**) qPCR data showing nascent SP100A RNA expression in ocular melanoma cells (92.1, OMM2.3 and CRMM1) upon ALKBH3 knockdown. The data are presented as the mean ± SD of experimental triplicates. Significance was determined by unpaired two-tailed Student’s t test.

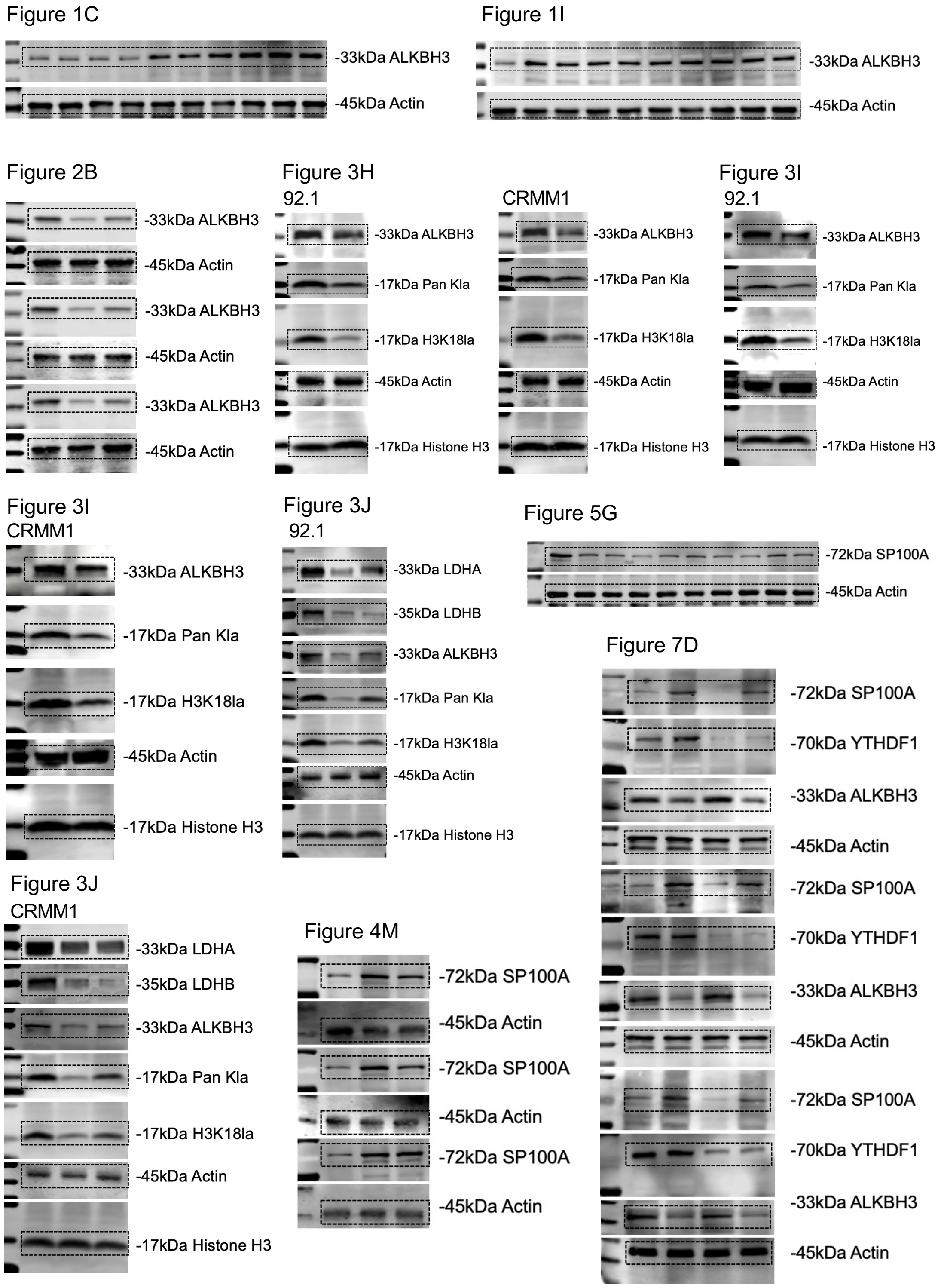

**Supplementary Figure S14. Unprocessed Western blot.**

Figure 5M

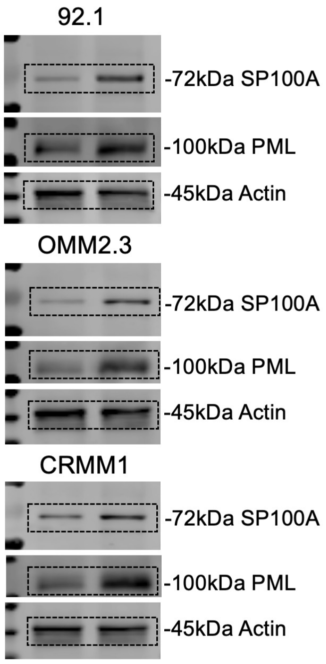

Figure 6F

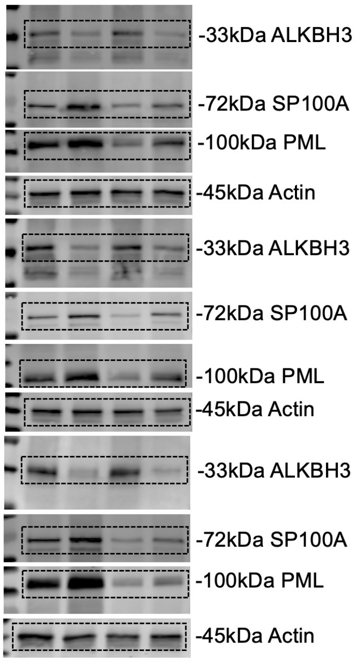

Supplementary Figure S9B

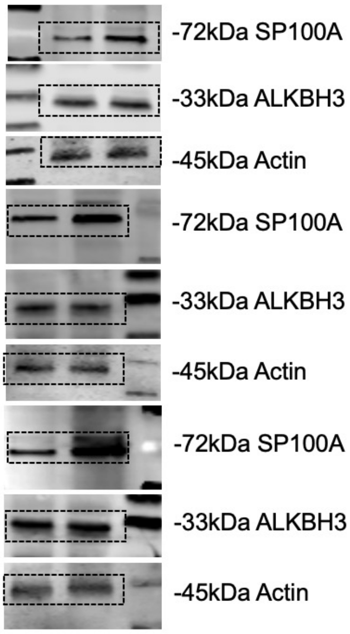

Supplementary Figure S11B

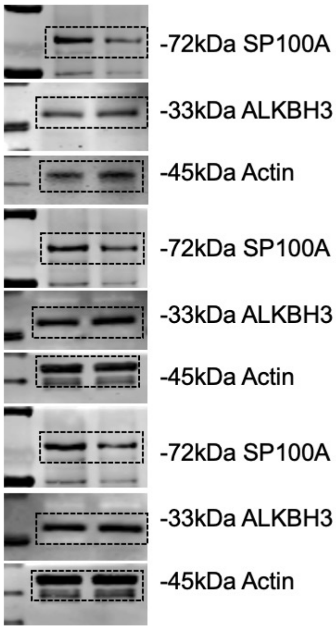

**Supplementary Figure S15. Unprocessed Western blot.**

**Supplementary Table S1. Primers and shRNAs sequences used in this study.**

| Primer name | Sequence (5'-3') | Purpose |
|---|---|---|
| ALKBH3-F | GCCACGAGTGATTGACAGAG | PCR |
| ALKBH3-R | ATGCGGTTCTTTAGTGTGCG | PCR |
| SP100-General-F | TAGGGTGGGAAGATGGCAGG | PCR |
| SP100-General-R | TGGTCTTCCGTGAACATCCTTT | PCR |
| SP100-P1-F | AAGCATGGTGAGAAGGCTCC | PCR |
| SP100-P1-R | CAAGTCTTGGCATCCTAATCTTCT | PCR |
| SP100-P2-F | GAAGAAAAGCCAACACTAGACCT | PCR |
| SP100-P2-R | ACACTTCTTTGAGGTTCCTTGT | PCR |
| YTHDF1-F | CGTGGACACCCAGAGAACAA | PCR |
| YTHDF1-R | TGCCCAAAAACAGCATCGTG | PCR |
| Fluc-F | CACCTTCGTGACTTCCCATT | PCR |
| Fluc-R | TGACTGAATCGGACACAAGC | PCR |
| ACTB-F | GATTCCTATGTGGGCGACGA | PCR |
| ACTB-R | AGGTCTCAAACATGATCTGGGT | PCR |
| a site-F | ACCTGGTAATTCAGCCCACAG | PCR |
| a site-R | CCTCTCAGCTGGCTCTTTAGT | PCR |
| b site-F | GATGTGGGACTACCCGGACT | PCR |
| b site-R | TTCCTCTCGACGTTACGCAG | PCR |
| c site-F | TTGCTGGAGTCGGTGCTTCA | PCR |
| c site-R | GCACCCAGCAGTAAGTCAGG | PCR |
| d site-F | TCCAAAGTTGGTGAGAGATGCT | PCR |
| d site-R | AGCCAATCTGCAAGCAGTCA | PCR |
| ALKBH3-shRNA1 | | shRNA |
| Sence | GGAACAGCTTTGTCAAGAT | |
| Antisence | ATCTTGACAAAGCTGTTCC | |
| ALKBH3-shRNA2 | | shRNA |
| Sence | GCACATTTGAGATGAGAAA | |
| Antisence | TTTCTCATCTCAAATGTGC | |
| SP100-shRNA | | shRNA |
| Sence | TGCGACTGGGTGATAAA | |
| Antisence | TTTATCACCCAGTCGCA | |
| YTHDF1-shRNA | | shRNA |
| Sence | GTTCGTTACATCAGAAGGATA | |
| Antisence | TATCCTTCTGATGTAACGAAC | |

**Supplementary Table S2. Oligonucleotides used for luciferase reporter gene.**

| Oligonucleotides name | Sequence (5’-3’) |
|---|---|
| *SP100*-5’UTR-WT | GCTTGGGGCC TGGGCAGCCA CACTGCACGC AGGCTGGGCC GACTGAGGGG CTCAGAGGCC AGGCTCTGAG GCCCACGCAG GGCCTAGGGT GGGAAG |
| *SP100*-5’UTR-MUT1 | GCTTGGGGCC TGGGCAGCCA CACTGCACGC AGGCTGGGCC GACTGTGGGG CTCAGAGGCC AGGCTCTGAG GCCCACGCAG GGCCTAGGGT GGGAAG |
| *SP100*-5’UTR-MUT2 | GCTTGGGGCC TGGGCAGCCA CACTGCACGC AGGCTGGGCC GACTGAGGGG CTCAGTGGCC AGGCTCTGAG GCCCACGCAG GGCCTAGGGT GGGAAG |
| *SP100*-5’UTR-MUT3 | GCTTGGGGCC TGGGCAGCCA CACTGCACGC AGGCTGGGCC GACTGAGGGG CTCAGAGGCC AGGCTCTGTG GCCCACGCAG GGCCTAGGGT GGGAAG |
| *SP100*-5’UTR-MUT4 | GCTTGGGGCC TGGGCAGCCA CACTGCACGC AGGCTGGGCC GACTGAGGGG CTCAGAGGCC AGGCTCTGAG GCCCACGCAG GGCCTAGGGT GGGTAG |
| *SP100*-5’UTR-MUT5 | GCTTGGGGCC TGGGCAGCCA CACTGCACGC AGGCTGGGCC GACTGAGGGG CTCAGAGGCC AGGCTCTGAG GCCCACGCAG GGCCTAGGGT GGGATG |
| *SP100*-5’UTR-MUT1-5 | GCTTGGGGCC TGGGCAGCCA CACTGCACGC AGGCTGGGCC GACTGTGGGG CTCAGTGGCC AGGCTCTGTG GCCCACGCAG GGCCTAGGGT GGGTTG |

## Supplementary Table S3. The differentially expressed proteins in proteomic analysis.

| Accession | Protein Name | Gene Name | SH-1/REF | SH-2/REF | NC-1/REF | NC-2/REF | SH/NC | Significance |
|---|---|---|---|---|---|---|---|---|
| Q969S2 | Endonuclease 8-like 2 | NEIL2 | 1.912 | 2.117 | 0.697 | 0.641 | 3.012 | 8.8506E-66 |
| Q10589 | Bone marrow stromal antigen 2 | BST2 | 1.829 | 1.845 | 0.646 | 0.653 | 2.828 | 1.0111E-58 |
| Q9UID6 | Zinc finger protein 639 | ZNF639 | 1.898 | 1.760 | 0.683 | 0.653 | 2.739 | 2.9252E-55 |
| Q8NHV4 | Protein NEDD1 | NEDD1 | 2.007 | 1.620 | 0.640 | 0.722 | 2.663 | 2.6016E-52 |
| Q8TCB0 | Interferon-induced protein 44 | IFI44 | 1.642 | 1.788 | 0.730 | 0.609 | 2.562 | 2.0799E-48 |
| O43462 | Membrane-bound transcription factor site-2 protease | MBTPS2 | 1.675 | 1.793 | 0.657 | 0.743 | 2.478 | 3.5979E-45 |
| O15162 | Phospholipid scramblase 1 | PLSCR1 | 1.748 | 1.535 | 0.637 | 0.716 | 2.427 | 3.3295E-43 |
| P29728 | 2'-5'-oligoadenylate synthase 2 | OAS2 | 1.525 | 1.533 | 0.699 | 0.682 | 2.215 | 4.1069E-35 |
| P09914 | Interferon-induced protein with tetratricopeptide repeats 1 | IFIT1 | 1.565 | 1.572 | 0.742 | 0.715 | 2.153 | 8.9941E-33 |
| O95786 | Antiviral innate immune response receptor RIG-I | DDX58 | 1.551 | 1.557 | 0.740 | 0.759 | 2.073 | 8.2424E-30 |
| O43805 | Sjoegren syndrome nuclear autoantigen 1 | SSNA1 | 1.538 | 1.620 | 0.827 | 0.781 | 1.964 | 8.5006E-26 |
| Q53G44 | Interferon-induced protein 44-like | IFI44L | 1.442 | 1.416 | 0.741 | 0.780 | 1.880 | 9.4151E-23 |
| Q9H8Y5 | Ankyrin repeat and zinc finger domain-containing protein 1 | ANKZF1 | 1.569 | 0.491 | 0.701 | 0.403 | 1.866 | 2.9177E-22 |
| P20592 | Interferon-induced GTP-binding protein Mx2 | MX2 | 1.454 | 1.399 | 0.778 | 0.764 | 1.851 | 9.8016E-22 |
| O14879 | Interferon-induced protein with tetratricopeptide repeats 3 | IFIT3 | 1.407 | 1.420 | 0.750 | 0.798 | 1.826 | 7.2535E-21 |
| Q9Y646 | Carboxypeptidase Q | CPQ | 1.383 | 1.421 | 0.765 | 0.778 | 1.817 | 1.4985E-20 |
| Q14703 | Membrane-bound transcription factor site-1 protease | MBTPS1 | 1.588 | 1.410 | 0.816 | 0.847 | 1.802 | 5.1234E-20 |
| Q8IVU3 | Probable E3 ubiquitin-protein ligase HERC6 | HERC6 | 1.295 | 1.568 | 0.728 | 0.879 | 1.781 | 2.5609E-19 |
| P42224 | Signal transducer and activator of transcription 1-alpha/beta | STAT1 | 1.396 | 1.373 | 0.757 | 0.800 | 1.778 | 3.3287E-19 |
| P13164 | Interferon-induced transmembrane protein 1 | IFITM1 | 1.440 | 1.366 | 0.786 | 0.811 | 1.757 | 1.7587E-18 |
| P01893 | Putative HLA class I histocompatibility antigen, alpha chain H | HLA-H | 1.632 | 1.270 | 0.814 | 0.864 | 1.731 | 1.3803E-17 |
| Q9H3M7 | Thioredoxin-interacting protein | TXNIP | 1.288 | 1.219 | 0.756 | 0.705 | 1.716 | 4.3601E-17 |
| Q01650 | Large neutral amino acids transporter small subunit 1 | SLC7A5 | 1.396 | 1.378 | 0.785 | 0.838 | 1.709 | 7.2459E-17 |
| Q8N1Q1 | Carbonic anhydrase 13 | CA13 | 1.458 | 1.376 | 0.874 | 0.808 | 1.686 | 4.3805E-16 |
| Q9NUL5 | Shiftless antiviral inhibitor of ribosomal frameshifting protein | SHFL | 1.321 | 1.395 | 0.756 | 0.860 | 1.681 | 6.256E-16 |
| Q9Y5U4 | Insulin-induced gene 2 protein | INSIG2 | 1.623 | 0.786 | 0.919 | 0.592 | 1.594 | 3.7021E-13 |
| O14933 | Ubiquitin/ISG15-conjugating enzyme E2 L6 | UBE2L6 | 1.338 | 1.290 | 0.816 | 0.834 | 1.593 | 4.0755E-13 |
| Q9Y6K5 | 2'-5'-oligoadenylate synthase 3 | OAS3 | 1.343 | 1.299 | 0.830 | 0.829 | 1.592 | 4.45E-13 |
| P05161 | Ubiquitin-like protein ISG15 | ISG15 | 1.342 | 1.246 | 0.816 | 0.818 | 1.583 | 8.6504E-13 |
| P07305 | Histone H1.0 | H1-0 | 1.363 | 1.326 | 0.859 | 0.864 | 1.561 | 4.0801E-12 |
| Q9P2W9 | Syntaxin-18 | STX18 | 1.304 | 1.416 | 0.882 | 0.865 | 1.557 | 5.1985E-12 |
| Q9Y3Z3 | Deoxynucleoside triphosphate triphosphohydrolase SAMHD1 | SAMHD1 | 1.323 | 1.309 | 0.860 | 0.830 | 1.556 | 5.5197E-12 |
| P52630 | Signal transducer and activator of transcription 2 | STAT2 | 1.316 | 1.299 | 0.835 | 0.849 | 1.552 | 7.3362E-12 |
| P10071 | Transcriptional activator GLI3 | GLI3 | 1.317 | 0.898 | 0.864 | 0.589 | 1.525 | 5.0324E-11 |
| Q9UDT6 | CAP-Gly domain-containing linker protein 2 | CLIP2 | 1.385 | 1.181 | 0.873 | 0.828 | 1.509 | 1.4185E-10 |
| P22694 | cAMP-dependent protein kinase catalytic subunit beta | PRKACB | 1.324 | 1.350 | 0.929 | 0.867 | 1.488 | 5.7645E-10 |

| | | | | | | | | |
|---|---|---|---|---|---|---|---|---|
| A6NEE1 | Pleckstrin homology domain-containing family D member 1 | PLEKHD1 | 1.331 | 1.287 | 0.886 | 0.883 | 1.480 | 1.0052E-09 |
| P27701 | CD82 antigen | CD82 | 1.296 | 1.334 | 0.868 | 0.912 | 1.477 | 1.2086E-09 |
| O00182 | Galectin-9 | LGALS9 | 1.299 | 1.244 | 0.845 | 0.887 | 1.469 | 2.0983E-09 |
| Q9BYC8 | 39S ribosomal protein L32, mitochondrial | MRPL32 | 1.284 | 1.232 | 0.840 | 0.874 | 1.468 | 2.2495E-09 |
| P23497 | Nuclear autoantigen Sp-100 | SP100 | 1.193 | 1.214 | 0.790 | 0.864 | 1.455 | 5.1131E-09 |
| Q5K651 | Sterile alpha motif domain-containing protein 9 | SAMD9 | 1.242 | 1.278 | 0.885 | 0.859 | 1.445 | 9.7342E-09 |
| Q53GL7 | Protein mono-ADP-ribosyltransferase PARP10 | PARP10 | 1.236 | 1.247 | 0.876 | 0.853 | 1.437 | 1.6012E-08 |
| Q9H930 | Nuclear body protein SP140-like protein | SP140L | 1.111 | 1.196 | 0.771 | 0.850 | 1.423 | 3.7864E-08 |
| Q96HD1 | Protein disulfide isomerase CRELD1 | CRELD1 | 1.269 | 1.181 | 0.839 | 0.895 | 1.412 | 7.3595E-08 |
| Q9NZT2 | Opioid growth factor receptor | OGFR | 1.327 | 1.282 | 0.997 | 0.850 | 1.412 | 7.4107E-08 |
| P01889 | HLA class I histocompatibility antigen, B alpha chain | HLA-B | 1.201 | 1.232 | 0.848 | 0.875 | 1.412 | 7.5318E-08 |
| Q460N5 | Protein mono-ADP-ribosyltransferase PARP14 | PARP14 | 1.279 | 1.217 | 0.923 | 0.857 | 1.402 | 1.3783E-07 |
| P39060 | Collagen alpha-1(XVIII) chain | COL18A1 | 1.274 | 1.200 | 0.872 | 0.904 | 1.393 | 2.3212E-07 |
| O14787 | Transportin-2 | TNPO2 | 1.211 | 1.282 | 0.852 | 0.951 | 1.383 | 4.2328E-07 |
| P13637 | Sodium/potassium-transporting ATPase subunit alpha-3 | ATP1A3 | 1.200 | 1.242 | 0.858 | 0.913 | 1.379 | 5.3381E-07 |
| P24385 | G1/S-specific cyclin-D1 | CCND1 | 0.939 | 1.730 | 0.652 | 1.285 | 1.378 | 5.7573E-07 |
| Q8IVG5 | Sterile alpha motif domain-containing protein 9-like | SAMD9L | 1.153 | 1.244 | 0.831 | 0.913 | 1.375 | 6.9157E-07 |
| P19525 | Interferon-induced, double-stranded RNA-activated protein kinase | EIF2AK2 | 1.216 | 1.201 | 0.870 | 0.891 | 1.373 | 7.5664E-07 |
| P55283 | Cadherin-4 | CDH4 | 1.190 | 1.362 | 0.845 | 1.017 | 1.370 | 8.8992E-07 |
| Q6PJF5 | Inactive rhomboid protein 2 | RHBDF2 | 1.001 | 1.015 | 0.688 | 0.784 | 1.369 | 9.3505E-07 |
| Q4L180 | Filamin A-interacting protein 1-like | FILIP1L | 1.231 | 1.402 | 0.828 | 1.109 | 1.360 | 1.6128E-06 |
| Q9Y6D5 | Brefeldin A-inhibited guanine nucleotide-exchange protein 2 | ARFGEF2 | 1.298 | 1.143 | 0.973 | 0.828 | 1.355 | 2.1178E-06 |
| Q5H9U9 | Probable ATP-dependent RNA helicase DDX60-like | DDX60L | 1.184 | 1.182 | 0.865 | 0.883 | 1.354 | 2.2198E-06 |
| P09913 | Interferon-induced protein with tetratricopeptide repeats 2 | IFIT2 | 1.207 | 1.224 | 0.893 | 0.903 | 1.354 | 2.2735E-06 |
| Q9UQ13 | Leucine-rich repeat protein SHOC-2 | SHOC2 | 1.210 | 1.100 | 0.833 | 0.883 | 1.347 | 3.356E-06 |
| O00469 | Procollagen-lysine,2-oxoglutarate 5-dioxygenase 2 | PLOD2 | 1.167 | 1.152 | 0.863 | 0.881 | 1.330 | 8.5902E-06 |
| Q06413 | Myocyte-specific enhancer factor 2C | MEF2C | 1.157 | 1.118 | 0.920 | 0.792 | 1.329 | 8.8432E-06 |
| O15460 | Prolyl 4-hydroxylase subunit alpha-2 | P4HA2 | 1.140 | 1.125 | 0.854 | 0.852 | 1.327 | 9.9144E-06 |
| P13726 | Tissue factor | F3 | 1.053 | 1.122 | 0.778 | 0.861 | 1.327 | 1.0143E-05 |
| O43294 | Transforming growth factor beta-1-induced transcript 1 protein | TGFB1I1 | 1.168 | 1.077 | 0.830 | 0.865 | 1.325 | 1.1173E-05 |
| Q5HYK7 | SH3 domain-containing protein 19 | SH3D19 | 1.096 | 1.151 | 0.861 | 0.842 | 1.319 | 1.5167E-05 |
| Q16666 | Gamma-interferon-inducible protein 16 | IFI16 | 1.210 | 1.172 | 0.911 | 0.902 | 1.314 | 2.0183E-05 |
| Q92522 | Histone H1.10 | H1-10 | 1.162 | 1.146 | 0.849 | 0.909 | 1.313 | 2.144E-05 |
| Q8IXQ6 | Protein mono-ADP-ribosyltransferase PARP9 | PARP9 | 1.223 | 1.150 | 0.856 | 0.952 | 1.313 | 2.1667E-05 |
| Q8IY21 | Probable ATP-dependent RNA helicase DDX60 | DDX60 | 1.222 | 1.197 | 0.930 | 0.914 | 1.312 | 2.2275E-05 |
| Q96A26 | Protein FAM162A | FAM162A | 1.128 | 1.118 | 0.841 | 0.873 | 1.310 | 2.4458E-05 |

| | | | | | | | | |
|---|---|---|---|---|---|---|---|---|
| P28838 | Cytosol aminopeptidase | LAP3 | 1.170 | 1.199 | 0.913 | 0.905 | 1.303 | 3.5315E-05 |
| P22415 | Upstream stimulatory factor 1 | USF1 | 0.810 | 1.593 | 0.883 | 0.973 | 1.295 | 5.4693E-05 |
| Q86YZ3 | Hornerin | HRNR | 1.531 | 0.871 | 1.268 | 0.588 | 1.294 | 5.5788E-05 |
| Q8IYM9 | E3 ubiquitin-protein ligase TRIM22 | TRIM22 | 1.204 | 1.192 | 0.927 | 0.925 | 1.293 | 5.8238E-05 |
| Q16877 | 6-phosphofructo-2-kinase/fructose-2,6-bisphosphatase 4 | PFKFB4 | 1.101 | 1.115 | 0.865 | 0.850 | 1.292 | 6.2261E-05 |
| P09543 | 2',3'-cyclic-nucleotide 3'-phosphodiesterase | CNP | 1.191 | 1.185 | 0.925 | 0.916 | 1.291 | 6.6511E-05 |
| Q9HB58 | Sp110 nuclear body protein | SP110 | 1.154 | 1.142 | 0.847 | 0.938 | 1.286 | 8.5215E-05 |
| P32455 | Guanylate-binding protein 1 | GBP1 | 1.204 | 1.170 | 0.929 | 0.920 | 1.284 | 9.1488E-05 |
| Q9ULC8 | Palmitoyltransferase ZDHHC8 | ZDHHC8 | 1.226 | 1.193 | 0.884 | 1.007 | 1.279 | 0.00011757 |
| P10321 | HLA class I histocompatibility antigen, C alpha chain | HLA-C | 1.207 | 1.158 | 0.903 | 0.946 | 1.279 | 0.00012131 |
| Q13077 | TNF receptor-associated factor 1 | TRAF1 | 1.172 | 1.183 | 0.918 | 0.930 | 1.275 | 0.00014625 |
| P61769 | Beta-2-microglobulin | B2M | 1.166 | 1.172 | 0.909 | 0.929 | 1.272 | 0.00017069 |
| Q00653 | Nuclear factor NF-kappa-B p100 subunit | NFKB2 | 1.251 | 1.155 | 0.970 | 0.922 | 1.272 | 0.00017249 |
| Q13207 | T-box transcription factor TBX2 | TBX2 | 1.029 | 1.056 | 0.791 | 0.850 | 1.271 | 0.00017667 |
| Q08380 | Galectin-3-binding protein | LGALS3BP | 1.159 | 1.137 | 0.905 | 0.904 | 1.269 | 0.00019502 |
| P13674 | Prolyl 4-hydroxylase subunit alpha-1 | P4HA1 | 1.133 | 1.118 | 0.906 | 0.868 | 1.269 | 0.00019965 |
| Q8IVF4 | Dynein heavy chain 10, axonemal | DNAH10 | 1.124 | 1.094 | 0.808 | 0.941 | 1.268 | 0.00020782 |
| Q8TDB6 | E3 ubiquitin-protein ligase DTX3L | DTX3L | 1.146 | 1.141 | 0.884 | 0.924 | 1.264 | 0.00024461 |
| P32321 | Deoxycytidylate deaminase | DCTD | 1.163 | 1.522 | 1.062 | 1.065 | 1.263 | 0.00026691 |
| P49840 | Glycogen synthase kinase-3 alpha | GSK3A | 1.059 | 1.527 | 1.020 | 1.029 | 1.263 | 0.00026729 |
| Q6KB66 | Keratin, type II cytoskeletal 80 | KRT80 | 1.140 | 1.118 | 0.891 | 0.901 | 1.261 | 0.00028757 |
| Q08AF3 | Schlafen family member 5 | SLFN5 | 1.185 | 1.144 | 0.920 | 0.927 | 1.261 | 0.00029293 |
| Q00403 | Transcription initiation factor IIB | GTF2B | 1.250 | 1.161 | 1.021 | 0.892 | 1.260 | 0.00029754 |
| P27797 | Calreticulin | CALR | 1.143 | 1.119 | 0.891 | 0.908 | 1.258 | 0.00033621 |
| Q96BY9 | Store-operated calcium entry-associated regulatory factor | SARAF | 1.129 | 1.281 | 0.892 | 1.026 | 1.256 | 0.00035886 |
| P51808 | Dynein light chain Tctex-type 3 | DYNLT3 | 1.209 | 1.037 | 0.921 | 0.868 | 1.256 | 0.0003655 |
| Q96BI3 | Gamma-secretase subunit APH-1A | APH1A | 1.089 | 1.141 | 0.860 | 0.917 | 1.255 | 0.00037835 |
| P50895 | Basal cell adhesion molecule | BCAM | 1.043 | 1.060 | 0.816 | 0.862 | 1.253 | 0.0004198 |
| Q9BTM9 | Ubiquitin-related modifier 1 | URM1 | 1.090 | 1.125 | 0.865 | 0.903 | 1.252 | 0.00042988 |
| P19474 | E3 ubiquitin-protein ligase TRIM21 | TRIM21 | 1.188 | 1.188 | 0.983 | 0.916 | 1.251 | 0.00046625 |
| Q9Y5W8 | Sorting nexin-13 | SNX13 | 1.121 | 1.127 | 0.866 | 0.932 | 1.250 | 0.00047661 |
| P62875 | DNA-directed RNA polymerases I, II, and III subunit RPABC5 | POLR2L | 1.216 | 1.860 | 1.322 | 1.141 | 1.249 | 0.0005112 |
| P78357 | Contactin-associated protein 1 | CNTNAP1 | 1.039 | 1.037 | 0.802 | 0.864 | 1.246 | 0.00059022 |
| Q9BYM8 | RanBP-type and C3HC4-type zinc finger-containing protein 1 | RBCK1 | 1.083 | 1.150 | 0.879 | 0.915 | 1.245 | 0.00061451 |
| P51787 | Potassium voltage-gated channel subfamily KQT member 1 | KCNQ1 | 1.154 | 1.043 | 0.850 | 0.916 | 1.244 | 0.00063286 |
| Q16875 | 6-phosphofructo-2-kinase/fructose-2,6-bisphosphatase 3 | PFKFB3 | 1.064 | 1.054 | 0.822 | 0.881 | 1.243 | 0.00066642 |
| Q07002 | Cyclin-dependent kinase 18 | CDK18 | 1.010 | 1.091 | 0.838 | 0.852 | 1.242 | 0.00068446 |
| Q9NUP1 | Biogenesis of lysosome-related organelles complex 1 subunit 4 | BLOC1S4 | 1.126 | 1.277 | 0.982 | 0.957 | 1.240 | 0.00078001 |
| Q9UL42 | Paraneoplastic antigen Ma2 | PNMA2 | 1.115 | 1.158 | 0.895 | 0.939 | 1.239 | 0.00079992 |
| Q6P2I3 | Fumarylacetoacetate hydrolase domain-containing protein 2B | FAHD2B | 1.155 | 1.148 | 0.939 | 0.919 | 1.239 | 0.00080612 |
| Q8WV24 | Pleckstrin homology-like domain family A member 1 | PHLDA1 | 1.189 | 1.044 | 0.922 | 0.883 | 1.238 | 0.00085143 |

| | | | | | | | | |
|---|---|---|---|---|---|---|---|---|
| Q9P225 | Dynein heavy chain 2, axonemal | DNAH2 | 1.114 | 1.044 | 0.843 | 0.901 | 1.237 | 0.00087615 |
| Q9NWZ5 | Uridine-cytidine kinase-like 1 | UCKL1 | 1.025 | 1.243 | 0.854 | 0.982 | 1.236 | 0.0009357 |
| Q8N5A5 | Zinc finger CCCH-type with G patch domain-containing protein | ZGPAT | 1.269 | 1.078 | 0.935 | 0.968 | 1.233 | 0.00103602 |
| O15182 | Centrin-3 | CETN3 | 1.131 | 1.042 | 0.959 | 0.804 | 1.233 | 0.00104692 |
| Q8TEP8 | Centrosomal protein of 192 kDa | CEP192 | 1.104 | 1.056 | 0.828 | 0.925 | 1.232 | 0.00109299 |
| Q86TB9 | Protein PAT1 homolog 1 | PATL1 | 1.115 | 1.254 | 0.945 | 0.980 | 1.231 | 0.00113932 |
| P29373 | Cellular retinoic acid-binding protein 2 | CRABP2 | 1.083 | 1.085 | 0.903 | 0.860 | 1.229 | 0.00122557 |
| P52746 | Zinc finger protein 142 | ZNF142 | 1.082 | 1.084 | 0.919 | 0.844 | 1.229 | 0.00126165 |
| Q8WUJ0 | Serine/threonine/tyrosine-interacting protein | STYX | 1.140 | 1.109 | 0.899 | 0.931 | 1.229 | 0.00127397 |
| Q06136 | 3-ketodihydrosphingosine reductase | KDSR | 1.188 | 1.073 | 0.886 | 0.956 | 1.227 | 0.00137184 |
| P11169 | Solute carrier family 2, facilitated glucose transporter member 3 | SLC2A3 | 1.083 | 1.139 | 0.885 | 0.927 | 1.226 | 0.00144317 |
| P55210 | Caspase-7 | CASP7 | 1.178 | 1.109 | 0.984 | 0.883 | 1.225 | 0.00147334 |
| P58335 | Anthrax toxin receptor 2 | ANTXR2 | 1.152 | 1.108 | 0.950 | 0.896 | 1.224 | 0.00152492 |
| P00558 | Phosphoglycerate kinase 1 | PGK1 | 1.117 | 1.085 | 0.918 | 0.882 | 1.224 | 0.0015584 |
| P00750 | Tissue-type plasminogen activator | PLAT | 1.148 | 1.168 | 0.983 | 0.910 | 1.224 | 0.00157773 |
| Q96BP3 | Peptidylprolyl isomerase domain and WD repeat-containing protein 1 | PPWD1 | 1.149 | 1.107 | 0.967 | 0.882 | 1.220 | 0.00184299 |
| Q9UBB9 | Tuftelin-interacting protein 11 | TFIP11 | 1.090 | 1.077 | 0.857 | 0.923 | 1.217 | 0.00206091 |
| Q9BQE5 | Apolipoprotein L2 | APOL2 | 1.145 | 1.141 | 0.930 | 0.948 | 1.217 | 0.00207378 |
| P35520 | Cystathionine beta-synthase | CBS | 1.024 | 1.147 | 0.769 | 1.015 | 1.217 | 0.00211945 |
| P24390 | ER lumen protein-retaining receptor 1 | KDELR1 | 0.940 | 0.896 | 0.796 | 0.714 | 1.215 | 0.00224457 |
| P04439 | HLA class I histocompatibility antigen, A alpha chain | HLA-A | 1.132 | 1.121 | 0.922 | 0.933 | 1.214 | 0.00237632 |
| P14921 | Protein C-ets-1 | ETS1 | 0.992 | 1.171 | 0.859 | 0.923 | 1.213 | 0.00245321 |
| Q92597 | Protein NDRG1 | NDRG1 | 1.093 | 0.959 | 0.862 | 0.830 | 1.213 | 0.00246538 |
| Q6IQ26 | DENN domain-containing protein 5A | DENND5A | 1.118 | 1.087 | 0.905 | 0.913 | 1.213 | 0.00249125 |
| Q13535 | Serine/threonine-protein kinase ATR | ATR | 1.008 | 1.028 | 0.826 | 0.854 | 1.212 | 0.00260054 |
| Q12882 | Dihydropyrimidine dehydrogenase [NADP(+)] | DPYD | 1.060 | 1.058 | 0.842 | 0.909 | 1.210 | 0.00284516 |
| Q9H5V8 | CUB domain-containing protein 1 | CDCP1 | 1.150 | 1.146 | 0.958 | 0.942 | 1.209 | 0.00299077 |
| Q8IVW4 | Cyclin-dependent kinase-like 3 | CDKL3 | 1.112 | 1.139 | 0.973 | 0.892 | 1.207 | 0.00318547 |
| Q06330 | Recombining binding protein suppressor of hairless | RBPJ | 1.201 | 1.030 | 0.954 | 0.897 | 1.205 | 0.00344695 |
| Q00978 | Interferon regulatory factor 9 | IRF9 | 1.142 | 1.129 | 1.005 | 0.881 | 1.204 | 0.00359849 |
| Q8NI22 | Multiple coagulation factor deficiency protein 2 | MCFD2 | 1.184 | 1.186 | 0.864 | 1.106 | 1.203 | 0.00377341 |
| Q96CU9 | FAD-dependent oxidoreductase domain-containing protein 1 | FOXRED1 | 1.133 | 1.117 | 0.847 | 1.025 | 1.202 | 0.0039371 |
| P06744 | Glucose-6-phosphate isomerase | GPI | 1.094 | 1.047 | 0.900 | 0.882 | 1.202 | 0.00395704 |
| P00973 | 2'-5'-oligoadenylate synthase 1 | OAS1 | 1.106 | 1.133 | 0.950 | 0.912 | 1.202 | 0.00396005 |
| Q8TBP5 | Membrane protein FAM174A | FAM174A | 1.049 | 1.028 | 0.910 | 0.818 | 1.202 | 0.003984 |
| Q9UL46 | Proteasome activator complex subunit 2 | PSME2 | 1.148 | 1.137 | 0.949 | 0.954 | 1.201 | 0.00410366 |
| Q9BU89 | Deoxyhypusine hydroxylase | DOHH | 0.928 | 0.936 | 1.173 | 1.064 | 0.833 | 0.00189316 |
| Q7Z6K5 | Arpin | ARPIN | 0.837 | 1.038 | 1.218 | 1.034 | 0.833 | 0.00185116 |
| O43715 | TP53-regulated inhibitor of apoptosis 1 | TRIAP1 | 0.911 | 0.903 | 1.122 | 1.060 | 0.831 | 0.00162177 |

| | | | | | | | | |
|---|---|---|---|---|---|---|---|---|
| Q8NB15 | Zinc finger protein 511 | ZNF511 | 0.841 | 0.922 | 1.033 | 1.089 | 0.831 | 0.00161237 |
| P20290 | Transcription factor BTF3 | BTF3 | 0.958 | 0.923 | 1.183 | 1.080 | 0.831 | 0.00160525 |
| Q9UG56 | Phosphatidylserine decarboxylase proenzyme, mitochondrial | PISD | 0.839 | 0.895 | 1.050 | 1.042 | 0.829 | 0.0014276 |
| P62304 | Small nuclear ribonucleoprotein E | SNRPE | 0.752 | 1.011 | 1.059 | 1.072 | 0.827 | 0.00123631 |
| Q96GC9 | Vacuole membrane protein 1 | VMP1 | 1.048 | 0.791 | 1.104 | 1.120 | 0.827 | 0.00119801 |
| Q6P582 | Mitotic-spindle organizing protein 2A | MZT2A | 0.821 | 0.928 | 1.097 | 1.022 | 0.825 | 0.00108134 |
| P13928 | Annexin A8 | ANXA8 | 0.892 | 0.953 | 1.137 | 1.101 | 0.825 | 0.00103341 |
| Q9NS87 | Kinesin-like protein KIF15 | KIF15 | 0.941 | 1.020 | 1.161 | 1.218 | 0.824 | 0.00099464 |
| P30838 | Aldehyde dehydrogenase, dimeric NADP-preferring | ALDH3A1 | 0.854 | 0.949 | 1.118 | 1.069 | 0.824 | 0.00098507 |
| P05204 | Non-histone chromosomal protein HMG-17 | HMGN2 | 0.907 | 0.887 | 1.131 | 1.046 | 0.824 | 0.00098362 |
| Q13765 | Nascent polypeptide-associated complex subunit alpha | NACA | 0.926 | 0.930 | 1.102 | 1.153 | 0.823 | 0.00090573 |
| Q9H4L7 | SWI/SNF-related matrix-associated actin-dependent regulator of chromatin subfamily A containing DEAD/H box 1 | SMARCAD1 | 0.909 | 0.991 | 1.015 | 1.298 | 0.821 | 0.00080888 |
| O14681 | Etoposide-induced protein 2.4 homolog | EI24 | 0.931 | 0.980 | 1.128 | 1.200 | 0.821 | 0.00076053 |
| Q86TS9 | 39S ribosomal protein L52, mitochondrial | MRPL52 | 0.944 | 0.882 | 1.236 | 0.991 | 0.820 | 0.00073702 |
| Q99595 | Mitochondrial import inner membrane translocase subunit Tim17-A | TIMM17A | 0.883 | 0.906 | 1.161 | 1.021 | 0.820 | 0.00072773 |
| Q8WV99 | AN1-type zinc finger protein 2B | ZFAND2B | 0.927 | 0.920 | 1.126 | 1.129 | 0.819 | 0.00066582 |
| Q3B726 | DNA-directed RNA polymerase I subunit RPA43 | POLR1F | 0.862 | 0.951 | 1.158 | 1.057 | 0.818 | 0.00064084 |
| P05090 | Apolipoprotein D | APOD | 1.010 | 0.937 | 1.202 | 1.186 | 0.815 | 0.00050602 |
| P59536 | Taste receptor type 2 member 41 | TAS2R41 | 0.767 | 0.884 | 0.939 | 1.087 | 0.815 | 0.00048377 |
| P98179 | RNA-binding protein 3 | RBM3 | 0.787 | 0.985 | 1.067 | 1.114 | 0.813 | 0.00040779 |
| O60613 | Selenoprotein F | SELENOF | 0.879 | 0.901 | 1.071 | 1.120 | 0.812 | 0.00039371 |
| Q5JV73 | FERM and PDZ domain-containing protein 3 | FRMPD3 | 0.857 | 0.818 | 1.097 | 0.967 | 0.812 | 0.00038427 |
| Q9NZP5 | Olfactory receptor 5AC2 | OR5AC2 | 0.843 | 0.837 | 1.033 | 1.038 | 0.812 | 0.0003755 |
| Q9H1E3 | Nuclear ubiquitous casein and cyclin-dependent kinase substrate 1 | NUCKS1 | 0.935 | 0.790 | 1.048 | 1.084 | 0.809 | 0.00030398 |
| Q96RS0 | Trimethylguanosine synthase | TGS1 | 0.814 | 1.008 | 1.109 | 1.150 | 0.806 | 0.00024603 |
| O75683 | Surfeit locus protein 6 | SURF6 | 0.828 | 0.954 | 1.135 | 1.075 | 0.806 | 0.00024345 |
| P63302 | Selenoprotein W | SELENOW | 0.903 | 0.872 | 1.076 | 1.126 | 0.806 | 0.00023548 |
| Q5TBB1 | Ribonuclease H2 subunit B | RNASEH2B | 0.877 | 0.925 | 1.115 | 1.128 | 0.804 | 0.00019192 |
| P05120 | Plasminogen activator inhibitor 2 | SERPINB2 | 0.959 | 0.955 | 1.198 | 1.187 | 0.802 | 0.00017517 |
| O15446 | DNA-directed RNA polymerase I subunit RPA34 | POLR1G | 0.961 | 0.994 | 1.289 | 1.148 | 0.802 | 0.00017492 |
| A4FU01 | Myotubularin-related protein 11 | MTMR11 | 0.796 | 1.057 | 1.140 | 1.172 | 0.801 | 0.00016125 |
| Q9UI32 | Glutaminase liver isoform, mitochondrial | GLS2 | 0.904 | 0.930 | 1.201 | 1.096 | 0.799 | 0.00012492 |
| O94972 | E3 ubiquitin-protein ligase TRIM37 | TRIM37 | 0.784 | 0.841 | 0.952 | 1.086 | 0.797 | 0.00011324 |
| Q14011 | Cold-inducible RNA-binding protein | CIRBP | 0.893 | 0.921 | 1.117 | 1.168 | 0.794 | 8.022E-05 |
| P52926 | High mobility group protein HMGI-C | HMGA2 | 0.984 | 0.911 | 1.205 | 1.189 | 0.792 | 6.7836E-05 |
| Q9Y487 | V-type proton ATPase 116 kDa subunit a2 | ATP6V0A2 | 0.831 | 0.803 | 1.035 | 1.032 | 0.790 | 6.0331E-05 |

| | | | | | | | | |
|---|---|---|---|---|---|---|---|---|
| Q96JA4 | Membrane-spanning 4-domains subfamily A member 14 | MS4A14 | 0.798 | 0.788 | 1.002 | 1.006 | 0.790 | 5.6149E-05 |
| Q8IWS0 | PHD finger protein 6 | PHF6 | 0.850 | 0.987 | 1.283 | 1.048 | 0.788 | 4.838E-05 |
| Q6NUP7 | Serine/threonine-protein phosphatase 4 regulatory subunit 4 | PPP4R4 | 0.838 | 0.785 | 1.043 | 1.016 | 0.788 | 4.7917E-05 |
| Q9Y2H5 | Pleckstrin homology domain-containing family A member 6 | PLEKHA6 | 0.851 | 0.867 | 1.087 | 1.095 | 0.787 | 4.5151E-05 |
| Q8WTV0 | Scavenger receptor class B member 1 | SCARB1 | 0.732 | 1.059 | 1.172 | 1.115 | 0.783 | 2.9577E-05 |
| O14569 | Cytochrome b561 domain-containing protein 2 | CYB561D2 | 0.840 | 0.863 | 1.116 | 1.065 | 0.781 | 2.4287E-05 |
| Q96J84 | Kin of IRRE-like protein 1 | KIRREL1 | 0.791 | 0.940 | 1.344 | 0.878 | 0.779 | 2.05E-05 |
| O60706 | ATP-binding cassette sub-family C member 9 | ABCC9 | 0.847 | 0.761 | 1.122 | 0.943 | 0.778 | 1.9117E-05 |
| Q9UMS0 | NFU1 iron-sulfur cluster scaffold homolog, mitochondrial | NFU1 | 0.900 | 0.934 | 1.274 | 1.091 | 0.776 | 1.461E-05 |
| Q08623 | Pseudouridine-5'-phosphatase | PUDP | 1.009 | 0.929 | 1.115 | 1.395 | 0.772 | 1.0329E-05 |
| Q99757 | Thioredoxin, mitochondrial | TXN2 | 1.016 | 0.849 | 1.240 | 1.176 | 0.772 | 9.946E-06 |
| Q5EBL4 | RILP-like protein 1 | RILPL1 | 0.874 | 0.966 | 1.222 | 1.178 | 0.766 | 5.5528E-06 |
| Q6PK04 | Coiled-coil domain-containing protein 137 | CCDC137 | 0.847 | 0.800 | 1.152 | 1.009 | 0.762 | 3.5866E-06 |
| Q9BV57 | 1,2-dihydroxy-3-keto-5-methylthiopentene dioxygenase | ADI1 | 0.848 | 0.845 | 1.147 | 1.089 | 0.757 | 2.0493E-06 |
| P47895 | Aldehyde dehydrogenase family 1 member A3 | ALDH1A3 | 0.809 | 0.809 | 1.077 | 1.089 | 0.747 | 5.977E-07 |
| Q8NC42 | E3 ubiquitin-protein ligase RNF149 | RNF149 | 0.778 | 0.798 | 1.064 | 1.128 | 0.719 | 1.6333E-08 |
| Q9BV44 | THUMP domain-containing protein 3 | THUMPD3 | 0.772 | 0.855 | 1.096 | 1.178 | 0.716 | 1.0562E-08 |
| Q8TCF1 | AN1-type zinc finger protein 1 | ZFAND1 | 0.709 | 0.884 | 1.098 | 1.158 | 0.706 | 2.6239E-09 |
| P13611 | Versican core protein | VCAN | 0.803 | 0.915 | 1.430 | 1.009 | 0.705 | 2.1293E-09 |
| Q68DU8 | BTB/POZ domain-containing protein KCTD16 | KCTD16 | 0.691 | 0.695 | 0.988 | 1.009 | 0.694 | 4.2849E-10 |
| Q9UPY5 | Cystine/glutamate transporter | SLC7A11 | 0.834 | 0.814 | 1.243 | 1.164 | 0.685 | 9.2888E-11 |
| Q13322 | Growth factor receptor-bound protein 10 | GRB10 | 0.722 | 0.755 | 0.904 | 1.259 | 0.683 | 6.8451E-11 |
| P07203 | Glutathione peroxidase 1 | GPX1 | 0.772 | 0.782 | 1.138 | 1.161 | 0.676 | 2.2474E-11 |
| O94808 | Glutamine--fructose-6-phosphate aminotransferase [isomerizing] 2 | GFPT2 | 0.672 | 0.625 | 1.033 | 0.923 | 0.663 | 2.0665E-12 |
| P02748 | Complement component C9 | C9 | 0.653 | 0.809 | 1.210 | 1.276 | 0.588 | 8.7947E-20 |
| Q9H6N6 | Putative uncharacterized protein MYH16 | MYH16 | 0.904 | 0.942 | 0.693 | 2.556 | 0.568 | 3.5002E-22 |
| O75629 | Protein CREG1 | CREG1 | 0.818 | 0.864 | 1.099 | 2.053 | 0.534 | 5.2491E-27 |
| O75764 | Transcription elongation factor A protein 3 | TCEA3 | 0.468 | 0.507 | 1.279 | 1.378 | 0.367 | 2.352E-66 |

**Supplementary Table S4. The clinical characteristics of ocular melanoma patient cohorts in tissue chip assay.**

| Patient No. | Gender (0=Female, 1=Male) | Age (years old) | Time for recurrence (month, 0=No recurrence) | Relative expression of ALKBH3 | Relative expression of SP100A |
|---|---|---|---|---|---|
| 1 | 1 | 59 | 2 | 0.3 | 0.5 |
| 2 | 1 | 59 | 2 | 6.2 | 1.3 |
| 3 | 1 | 45 | / | 7.5 | 0.8 |
| 4 | 1 | 45 | / | 1.2 | 3.3 |
| 5 | 1 | 57 | / | 2.0 | 4.2 |
| 6 | 1 | 54 | 36 | 1.2 | 1.3 |
| 7 | 1 | 54 | 6 | 2.3 | 1.1 |
| 8 | 1 | 76 | 0 | 0.5 | 0.4 |
| 9 | 0 | 54 | 0 | 2.8 | 1.8 |
| 10 | 1 | 46 | 6 | 5.4 | 0.5 |
| 11 | 1 | 57 | 24 | 2.3 | 0.9 |
| 12 | 1 | 57 | 24 | 0.6 | 0.9 |
| 13 | 1 | 67 | / | 2.8 | 1.1 |
| 14 | 1 | 59 | 2 | 2.0 | 0.3 |
| 15 | 1 | 59 | 2 | 0.8 | 0.2 |
| 16 | 0 | 89 | 0 | 1.1 | 2.3 |
| 17 | 0 | 89 | 0 | 0.9 | 1.5 |
| 18 | 1 | 52 | / | 2.9 | 1.0 |
| 19 | 1 | 37 | / | 3.3 | 1.1 |
| 20 | 1 | 82 | 0 | 2.1 | 1.4 |
| 21 | 1 | 82 | 0 | 1.3 | 2.8 |
| 22 | 1 | 48 | 60 | 0.7 | 0.3 |
| 23 | 0 | 29 | 0 | 0.4 | 0.3 |
| 24 | 0 | 49 | 11 | 3.1 | 0.6 |
| 25 | 0 | 49 | 11 | 5.3 | 0.2 |
| 26 | 1 | 35 | 34 | 0.8 | 1.4 |
| 27 | 1 | 35 | 34 | 1.0 | 1.2 |
| 28 | 1 | 47 | 0 | 1.8 | 2.5 |
| 29 | 0 | 60 | / | 2.4 | 1.1 |
| 30 | 1 | 64 | / | 1.6 | 0.8 |
| 31 | 1 | 52 | 2 | 6.6 | 0.2 |
| 32 | 0 | 77 | 19 | 5.8 | 0.9 |
| 33 | 0 | 45 | / | 7.9 | 1.0 |
| 34 | 0 | 42 | 18 | 1.9 | 1.0 |
| 35 | 1 | 55 | 12 | 4.2 | 1.2 |

| | | | | | |
|---|---|---|---|---|---|
| 36 | 1 | 65 | / | 4.9 | 2.4 |
| 37 | 1 | 61 | 3 | 3.1 | 0.2 |
| 38 | 1 | 31 | 13 | 1.2 | 0.9 |
| 39 | 1 | 32 | / | 2.0 | 1.4 |
| 40 | 0 | 66 | / | 2.5 | 1.6 |
| 41 | 0 | 69 | / | 2.1 | 1.5 |
| 42 | 0 | 31 | 3 | 2.3 | 1.1 |
| 43 | 1 | 13 | / | 2.2 | 1.5 |
| 44 | 1 | 64 | / | 1.6 | 0.7 |
| 45 | 0 | 67 | 0 | 1.7 | 3.8 |
| 46 | 1 | 23 | / | 2.5 | 0.9 |
| 47 | 1 | 23 | / | 2.3 | 0.9 |
| 48 | 1 | 52 | 0 | 2.0 | 2.3 |
| 49 | 1 | 12 | / | 1.4 | 0.8 |
| 50 | 1 | 73 | 13 | 0.6 | 0.2 |
| 51 | 0 | 52 | / | 2.5 | 0.5 |
| 52 | 1 | 31 | 13 | 3.3 | 1.1 |
| 53 | 1 | 78 | 0 | 0.4 | 1.8 |
| 54 | 0 | 42 | 18 | 4.1 | 0.9 |
| 55 | 1 | 66 | 20 | 1.5 | 0.5 |
| 56 | 1 | 58 | 0 | 7.4 | 0.9 |
| 57 | 0 | 82 | / | 1.4 | 2.6 |
| 58 | 1 | 80 | / | 1.9 | 1.0 |
| 59 | 1 | 73 | / | 2.0 | 0.7 |
| 60 | 1 | 60 | 9 | 1.9 | 0.7 |
| 61 | 0 | 51 | 12 | 3.4 | 0.8 |
| 62 | 0 | 58 | / | 2.4 | 1.7 |
| 63 | 1 | 52 | 2 | 7.4 | 0.2 |
| 64 | 1 | 73 | 13 | 4.8 | 1.1 |
| 65 | 1 | 81 | 0 | 3.2 | 1.3 |
| 66 | 1 | 20 | / | 1.7 | 0.9 |
| 67 | 1 | 47 | 16 | 3.2 | 1.3 |
| 68 | 0 | 77 | 19 | 4.6 | 1.3 |
| 69 | 1 | 54 | 2 | 1.9 | 0.3 |
| 70 | 1 | 63 | 32 | 1.2 | 0.4 |
| 71 | 1 | 38 | 8 | 5.2 | 0.9 |
| 72 | 1 | 38 | 8 | 3.4 | 0.1 |
| 73 | 1 | 70 | 23 | 1.3 | 0.8 |
| 74 | 1 | 70 | 23 | 1.2 | 0.3 |
| 75 | 1 | 18 | 6 | 2.4 | 0.1 |
| 76 | 1 | 18 | 6 | 0.6 | 0.3 |

| | | | | | |
|---|---|---|---|---|---|
| 77 | 1 | 76 | 0 | 1.5 | 1.4 |
| 78 | 1 | 75 | 0 | 1.6 | 1.5 |
| 79 | 0 | 53 | 5 | 6.1 | 0.3 |
| 80 | 1 | 74 | 0 | 5.7 | 0.7 |
| 81 | 1 | 49 | 0 | 0.8 | 0.6 |
| 82 | 1 | 67 | 0 | 0.6 | 0.4 |

**Supplementary Table S5. The clinical characteristics of melanocytic nevus patient cohorts in tissue chip assay.**

| Patient No. | Gender (0=Female, 1=Male) | Age (years old) | Relative expression of ALKBH3 | Relative expression of SP100A |
|---|---|---|---|---|
| 1 | 1 | 64 | 0.3 | 1.3 |
| 2 | 0 | 48 | 0.8 | 0.8 |
| 3 | 0 | 29 | 0.8 | 1.6 |
| 4 | 0 | 29 | 0.4 | 1.4 |
| 5 | 1 | 31 | 0.3 | 2.6 |
| 6 | 0 | 25 | 0.3 | 1.5 |
| 7 | 1 | 32 | 1.0 | 0.7 |
| 8 | 0 | 65 | 0.9 | 5.5 |
| 9 | 0 | 61 | 0.5 | 1.3 |
| 10 | 1 | 55 | 0.4 | 0.8 |
| 11 | 0 | 30 | 0.4 | 4.2 |
| 12 | 1 | 50 | 0.3 | 1.3 |
| 13 | 1 | 67 | 0.3 | 5.1 |
| 14 | 1 | 40 | 0.4 | 4.3 |
| 15 | 0 | 31 | 0.4 | 0.4 |
| 16 | 0 | 54 | 0.4 | 1.9 |
| 17 | 0 | 60 | 0.7 | 1.2 |
| 18 | 1 | 62 | 0.7 | 1.4 |
| 19 | 0 | 45 | 0.4 | 3.3 |
| 20 | 0 | 62 | 1.6 | 1.6 |
| 21 | 0 | 63 | 0.9 | 1.2 |
| 22 | 0 | 1 | 0.8 | 0.9 |
| 23 | 0 | 8 | 2.9 | 1.0 |
| 24 | 0 | 29 | 1.3 | 3.9 |
| 25 | 0 | 29 | 0.7 | 5.9 |
| 26 | 1 | 3 | 2.0 | 0.6 |
| 27 | 0 | 26 | 0.8 | 1.1 |
| 28 | 1 | 14 | 0.9 | 2.3 |

**Supplementary Table S6. The clinical characteristics of patients with high and low ALKBH3 levels.**

| Stratified by ALKBH3 | | | |
|---|---|---|---|
| | high | low | p-value |
| n | 29 | 29 | |
| age (mean (SD)) | 54.1 (15.4) | 59.2 (18.3) | 0.256 |
| sex = male (%) | 20 (69.0) | 24 (82.8) | 0.220 |
| T stage (%) | | | 0.452 |
| T1 | 1 (3.4) | 1 (3.4) | |
| T2 | 10 (34.5) | 13 (44.8) | |
| T3 | 18 (62.1) | 15 (51.7) | |

**Supplementary Table S7. The clinical characteristics of patients with high and low SP100A levels.**

| Stratified by SP100A | | | |
|---|---|---|---|
| | high | low | p-value |
| n | 29 | 29 | |
| age (mean (SD)) | 58.3 (18.7) | 55.1 (15.2) | 0.481 |
| sex = male (%) | 21 (72.4) | 23 (79.3) | 0.539 |
| T stage (%) | | | 0.979 |
| T1 | 2 (4.5) | 0 (0) | |
| T2 | 10 (34.5) | 13 (44.8) | |
| T3 | 17 (58.6) | 16 (55.2) | |